

Femtosecond sum frequency generation at the metal–liquid interface

Sylvie Roke^{a,*}, Aart W. Kleyn^{a,b}, Mischa Bonn^{a,c}

^a *Leiden Institute of Chemistry, P.O. Box 9502, 2300 RA Leiden, The Netherlands*

^b *FOM-Institute Rijnhuizen, P.O. Box 1207, 3430 BE Nieuwegein, The Netherlands*

^c *FOM-Institute AMOLF, Kruislaan 407, 1089 SJ Amsterdam, The Netherlands*

Available online 18 July 2005

Abstract

We present a study of the C–H and C–N vibrational modes of acetonitrile molecules at the interface between the bulk liquid and a gold film using both time and frequency domain femtosecond sum frequency generation. Acetonitrile is adsorbed on the gold surface with the N atom towards the interface. Due to the surface roughness there are different adsorption sites, leading to an inhomogeneous distribution of vibrational frequencies of the C–N stretch vibration of different molecules. This is observed most clearly in the time domain SFG measurements, while the frequency domain measurements are much less sensitive to the inhomogeneity. In contrast to the C–N stretch mode, the C–H stretching modes are unaffected by the surface and display homogeneous line broadening.

© 2005 Elsevier B.V. All rights reserved.

Keywords: Non-linear optical method; Sum frequency generation; Vibrations of adsorbed molecules; Gold; Solid–liquid interfaces

1. Introduction

Interfaces and surfaces play an important role in many chemical and physical processes occurring, for example, in heterogeneous catalysis and electrochemistry [1–3]. In many of these processes, the vibrational degrees of freedom of the molecules involved play a key role. The study of vibrational

dynamics of molecules at surfaces requires a technique that specifically probes vibrations of molecules at the interface, with sufficient time resolution to resolve the dynamics (occurring typically on a sub-picosecond time scale). As a second-order non-linear optical tool, femtosecond vibrational sum frequency generation (SFG) is ideally suited for this purpose [4].

In a vibrational SFG experiment an interface is probed by simultaneous (non-linear) interaction of an infrared (IR) and a visible (VIS) photon with the surface region. This results in the generation

* Corresponding author. Fax: +31 715274451.

E-mail addresses: roke@mf.mpg.de (S. Roke), bonn@amolf.nl (M. Bonn).

of a third photon, with the sum of the two frequencies. When the infrared field is resonant with a vibrational mode of a molecule at the surface, a resonant infrared polarization (\mathbf{P}_{IR}) is created, with a magnitude determined by the transition dipole moment (μ) and the infrared field. The infrared polarization decays in time, a process called the Free Induction Decay (FID), and is upconverted by the visible field in an SFG experiment. Due to the resonant excitation of molecular vibrations, the resulting sum frequency field is resonantly enhanced and contains information about the surface molecular vibrations.

In the experiments described here, we have used two different ways of performing SFG using femtosecond pulses, one to obtain time resolution and one to obtain frequency resolution. The first is performed using temporally short infrared and visible pulses (~ 100 fs). By delaying the pulses with respect to each other (see Fig. 1), the temporal decay of the resonant vibrational polarization can be followed in real-time [5–7]. The decay oc-

curs typically on a ~ 1 ps time scale. Although very high time resolution can be obtained in this approach, no frequency resolution can be achieved because both pulses have a large frequency content.

The second way—with very good frequency resolution—relies on combining a short infrared pulse with a long visible pulse (with a narrow frequency spectrum). As a consequence, the frequency distribution of the vibrationally enhanced SFG light is determined by the vibrational distribution, so that high frequency resolution is achieved. These two complementary approaches allow us to obtain information about the binding site (through the resonance frequency) and follow the vibrational dynamics of the polarization in real time.

In this article, we use time and frequency domain sum frequency generation to study acetonitrile (CH_3CN) molecules from the liquid phase adsorbed on a very thin gold film. We show that although both time and frequency domain mea-

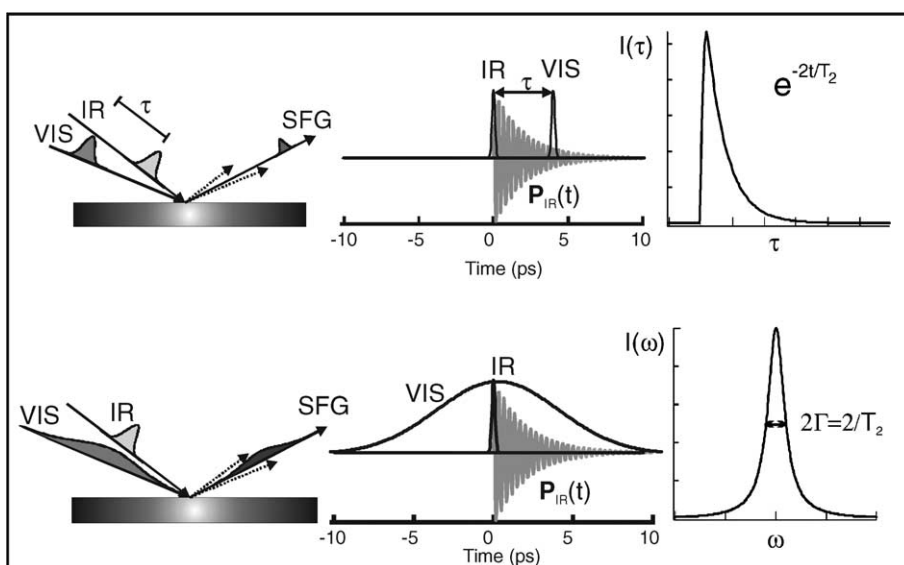


Fig. 1. Schematic illustration of a time domain (top) and a frequency domain (bottom) SFG experiment. In the time domain experiment, short pulses are employed, delayed by τ and the frequency-integrated SFG signal is recorded as a function of delay time between the infrared and visible pulses. In a frequency domain experiment, temporally long (spectrally narrow) visible pulses are used to upconvert the infrared-induced polarization at the surface and the time integrated signal is recorded as a function of frequency. The pictures in the middle panel illustrate the sequence of events in the time domain, showing the induced infrared polarization ($P_{\text{IR}}(t)$) that decays with a time constant T_2 and is upconverted by the visible pulse. The right panel displays the measured intensity in both scenarios.

measurements are theoretically equivalent, the time domain experiments are more sensitive to the inhomogeneity of adsorption sites, since the decay of the vibrational polarization can be mapped directly. We start (in Section 2) with a theoretical analysis necessary to model time and frequency domain sum frequency generation. From analysis of the vibrational CH₃ (in Section 4) and C–N stretch modes (in Section 5) we find that the surface roughness results in inhomogeneity in the vibrational C–N stretch mode, which is closest to the surface, but not in the C–H stretching mode, which is removed from the surface by an additional chemical bond. A generalization of the existing models allows for the simultaneous description of both frequency and time domain measurements.

2. Theoretical background

In a broad-band SFG experiment a broad-band femtosecond infrared pulse (\mathbf{E}_2 , containing frequencies ω_2) interacts resonantly with a vibrational mode of the adsorbed molecules. This induces a vibrational polarization (\mathbf{P}_{IR}) at the interface, which subsequently decays with a typical time constant T_2 , the dephasing time. This infrared polarization is upconverted by the visible field (containing frequencies ω_1) to create a second-order non-linear polarization $\mathbf{P}^{(2)}$ that oscillates at the sum frequency ($\omega_0 = \omega_1 + \omega_2$). The emitted electric field can be calculated by solving the Maxwell equations using $\mathbf{P}^{(2)}$ as a source term.

In a time domain experiment both IR and VIS pulses are short (~ 100 fs) and the SFG intensity (I_0) is recorded as a function of delay time (τ) between the two pulses (see the illustration in Fig. 1). The intensity is given by the following expression:

$$I_0(\tau) \propto \int_{-\infty}^{\infty} dt |\mathbf{P}^{(2)}(t, \tau)|^2 = \int_{-\infty}^{\infty} dt |\mathbf{P}_{\text{RES}}^{(2)}(t, \tau) + \mathbf{P}_{\text{NR}}^{(2)}(t, \tau)|^2 \quad (1)$$

in which the second-order non-linear polarization, $\mathbf{P}^{(2)}$, consists of the resonant response of the molecules, $\mathbf{P}_{\text{RES}}^{(2)}$, and the non-resonant response of

the metal, $\mathbf{P}_{\text{NR}}^{(2)}$. The second-order non-linear polarization for a single resonance and a given polarization combination of fields can be written as follows [8]:

$$P^{(2)}(t, \tau) = \bar{E}_1(t - \tau) \left\{ \int_{-\infty}^t A_{\text{RES}} \bar{E}_2(t') \bar{\chi}_{\text{RES}}^{(2)}(t - t') dt' + A_{\text{NR}} \bar{E}_2(t) e^{i\phi} \right\} e^{i(\omega_1 + \omega_2)t}, \quad (2)$$

where \bar{E}_1 and \bar{E}_2 are the envelopes of the visible and infrared fields. The first term of $P^{(2)}(t, \tau)$ describes the resonant response (with amplitude A_{RES}) of the adsorbate to the IR field. Integration in Eq. (2) over the dummy variable t' is necessary to incorporate the non-instantaneous response of the molecules to the incoming IR field. The second term in Eq. (2) describes the non-resonant (instantaneous) contribution from the metal with amplitude A_{NR} . The value of A_{RES} is determined by the magnitude of the infrared transition dipole moment and the Raman polarizability and A_{NR} is governed by the magnitude of the non-resonant hyperpolarizability. ϕ is the phase difference between the resonant and the non-resonant field and is approximated by a constant [9,10]. $\bar{\chi}_{\text{RES}}^{(2)}(t)$ is the envelope of $\chi_{\text{RES}}^{(2)}(t)$, which is usually modeled as [11–13]:

$$\chi_{\text{RES}}^{(2)}(t) = e^{-t/T_2} e^{i\omega_{0n}t}, \quad (3)$$

where ω_{0n} is the resonance frequency and T_2 is the dephasing time corresponding to vibrational mode n . This implies that all the molecules in the ensemble oscillate with the same frequency ω_{0n} , until they decay or lose mutual coherence due to dynamic effects (homogeneous dephasing). Such a distribution is called an homogeneous distribution [14]. Until now, the above description has proven sufficient to model the SFG spectra for an ensemble of molecules on a metal surface.

In a frequency domain experiment the IR polarization is the same as for a time domain experiment, but the upconversion occurs with a temporally long (and spectrally narrow) visible pulse to achieve high frequency resolution [15,16]. The measurement is performed in the frequency domain and the SFG intensity is more conveniently expressed in terms of the frequency domain

polarization. The latter is simply the Fourier transform of the time domain second-order non-linear polarization. Thus, time and frequency domain SFG experiments are in theory equivalent. This leads to the following equation to model frequency domain SFG measurements:

$$I_0(\omega) \propto \left| \frac{1}{\sqrt{2\pi}} \int_{-\infty}^{\infty} dt e^{i\omega t} P^{(2)}(t, \tau = 0) \right|^2 = |P^{(2)}(\omega)|^2 \quad (4)$$

with $P^{(2)}(t, \tau = 0)$ given by Eq. (1). Assuming a δ -function distribution (in the time domain) for the IR field, we have for the polarization [8]:

$$\begin{aligned} P^{(2)}(\omega_0 = \omega_1 + \omega_2) &= \chi^{(2)}(\omega_0 = \omega_1 + \omega_2) \\ &\times E_1(\omega_1)E_2(\omega_2) \quad \text{with} \\ \chi^{(2)}(\omega) &= A_{\text{RES}}\chi_{\text{RES}}^{(2)}(\omega) + A_{\text{NR}}\chi_{\text{NR}}^{(2)} \\ &= \frac{A_{\text{RES}}}{(\omega - \omega_{0m}) + i\Gamma} + A_{\text{NR}}e^{i\phi}, \end{aligned} \quad (5)$$

where $\Gamma = 1/T_2$. For a zero non-resonant contribution this results in a Lorentzian line shape with a FWHM of 2Γ (see Fig. 1). However, if there is both a resonant and a non-resonant contribution to the signal the line shape becomes distorted and critically depends on the phase factor ϕ . This can result in a large variety of line shapes (see, e.g., [9]).

If the duration of the visible pulse is comparable to or shorter than the decay time of the polarization (i.e. the linewidths of the visible pulse and the resonant intensity are comparable), the spectral lines can appear broader (or narrower, depending on the pulse timing) than the actual vibrational resonance [9,17,18]. To partially account for these effects, the second-order non-linear susceptibility may be convoluted with the visible field.

3. Experimental

The SFG experiments are performed using 120 fs FWHM Gaussian pulse duration infrared pulses (10 μJ energy; FWHM spectral bandwidth of 220 cm^{-1}) centered at 2940 cm^{-1} and 2250 cm^{-1} for investigating the C–H and C–N stretch

mode of acetonitrile, respectively. The temporal and spectral profile of the 800 nm visible pulse (2.3 μJ , repetition rate reduced from 1 kHz to 83 Hz) was varied using a pulse-shaper: frequency domain SFG spectra are recorded with a 3 cm^{-1} FWHM bandwidth (>10 ps auto-correlate width) upconversion pulse and time domain FIDs are measured with 120 fs visible pulses. Switching from time domain to frequency domain measurements only requires the insertion of a slit in the pulse-shaper, leaving the alignment unchanged. For a meaningful comparison, we have used identical energies of the visible pulse in the frequency domain and time domain experiments. Note that it is straightforward to increase the signal in the time domain measurement, by increasing the pulse energy. In the frequency domain measurement, increasing the pulse energy cannot be done without sacrificing spectral resolution, for our type of experimental set-up. The measurements were done in a co-propagating total internal reflection geometry (after [10,19]) in which the reflected SFG field is detected (see Fig. 2). In this geometry, the fields at the interface (a rough metal surface on top of a dielectric prism) become enhanced, leading to a large SFG signal [9,19]. The p-polarized IR and VIS pulses are incident under angles of 57° and 61° with respect to the surface normal, respectively. Infrared spectra of liquid acetonitrile (spectroscopic grade) are taken (at 2 cm^{-1} resolution) with a Biorad FTS 175 FTIR spectrometer. Gold films of ~ 3 nm thickness are prepared by evaporating gold from a filament on the back of a 60° CaF_2 prism. This produces films with a roughness determined by the substrate. Fig. 2 shows an AFM picture of a freshly evaporated 3 nm thick gold film on the back of a CaF_2 prism. This picture clearly shows the roughness of the gold surface. By reducing the repetition rate (with a phase-locked optical chopper) to 83 Hz, the thermal load was kept sufficiently low in order to avoid damage. The absorbed fluence was kept well below the ablation threshold $\sim 1.7 \text{ mJ}/\text{cm}^2$, as determined both experimentally and from a two temperature model calculation (see, e.g., [20]). Prior to each measurement the signal of the non-resonant $\text{CaF}_2/\text{gold}/\text{air}$ interface was checked to make sure that the layer was not damaged. The signal of a

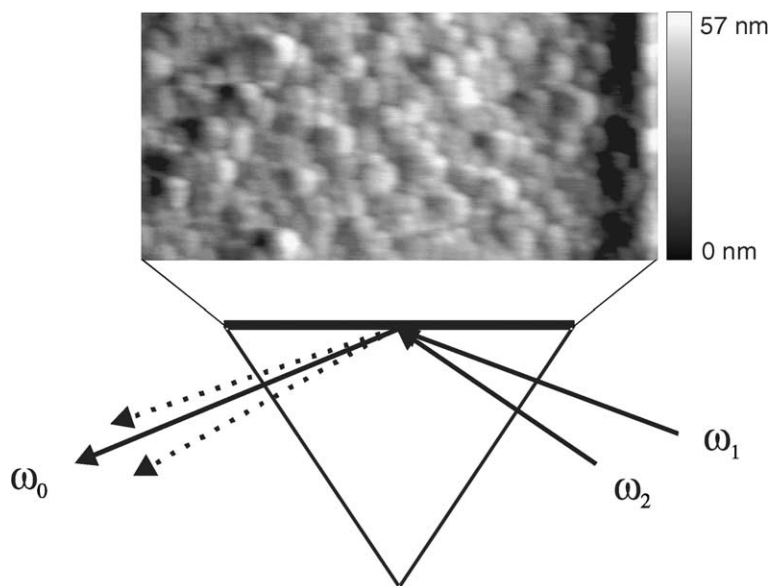


Fig. 2. Schematic illustration of the co-propagating optical geometry with an AFM picture ($400 \text{ nm} \times 200 \text{ nm}$) of a 3 nm thick gold film on the back of the CaF_2 prism. The root mean square roughness is 6.6 nm.

purposely damaged gold layer is dramatically (more than 2 orders of magnitude) lower. Thus it was ensured that the experiments presented here were performed on intact gold layers. The morphology of our gold surface closely resembles that used by Williams et al. [10] in their SFG study of adsorbates on gold. They were not able to perform total internal reflection measurements on layers with a thickness less than 5 nm, due to single-pulse damage. It is possible in our experiments to use films as thin as 3 nm, however, because our visible pulses are appreciably shorter than 4 ns. These short pulses can deliver high intensities required for SFG in combination with a relatively small heat load.

4. Homogeneous broadening

Fig. 3 depicts frequency domain SFG spectra in the C–H stretch region of acetonitrile, for the bare gold surface and for the surface in contact with acetonitrile. Two resonant features can be observed for the latter, one at 2939 cm^{-1} corresponding to the symmetric stretch vibration and a weak,

but clearly visible, feature at 3000 cm^{-1} , which can be attributed to the asymmetric stretch vibration. The fit in the frequency domain data in Fig. 3 is obtained by employing Eqs. (4) and (5) using the non-resonant contribution from the gold/air SFG spectrum and results in a dephasing time of 0.66 ps ($\Gamma = 8.0 \pm 0.2 \text{ cm}^{-1}$) for the symmetric stretch vibration and a dephasing time of 0.30 ps ($\Gamma = 18 \pm 0.7 \text{ cm}^{-1}$) for the asymmetric stretch vibration. Such a fast dephasing of the C–H symmetric stretch is comparable to the dephasing time of the same mode in other systems, like a self-assembled monolayer of ferric stearate on CaF_2 (0.59 ps) [21], acetonitrile on YAG (0.42 ps) [22] or acetonitrile on ZrO_2 [19] ($\Gamma = 5.7 \text{ cm}^{-1}$, corresponding to $T_2 = 0.93 \text{ ps}$). The bottom panel of Fig. 3 shows the time domain SFG measurements (the free induction decay (FID)) of the symmetric C–H stretch vibration. Also shown is a measurement of the gold/air interface, which is the cross-correlate of the IR and VIS pulses. It allows for the determination of the time resolution in the measurements (FWHM: 220 fs). From the linear decay on the log-normal scale, it is clear that the vibrational polarization of the C–H stretch mode

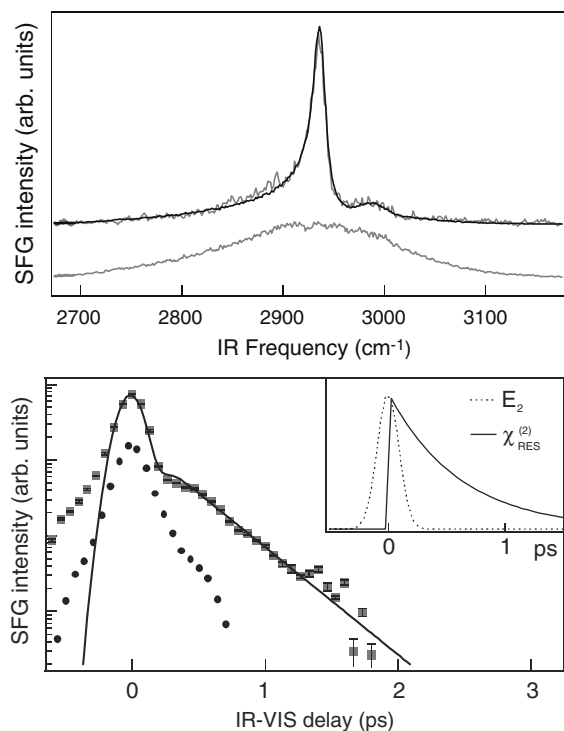


Fig. 3. Top panel: SFG spectra in the C–H stretch region of a gold film in contact with acetonitrile. The black line is a fit using Eqs. (4) and (5). The gold/air SFG spectrum is also shown. Bottom panel: Free induction decay (on a log-normal scale) of the C–H stretch vibration. A cross-correlate generated at the gold/air interface is also shown. The solid line is a fit using Eqs. (1)–(3) (assuming a single resonance frequency for the entire ensemble). The inset shows the functional form of the IR field envelope in combination with the envelope of the resonant second-order susceptibility used in the fit procedure.

decays exponentially. Thus, the C–H stretch mode is homogeneously broadened. The fit was obtained using Eqs. (1)–(3) with a dephasing time of 0.61 ps. This value compares favorably to the value of 0.66 ps deduced from frequency domain data. It shows that both time and frequency domain data are in good correspondence with each other. This is required, since in both schemes the polarization decay is detected. (Note that the relative phase ϕ can be different however, as the visible pulse passes through some attenuating optics in the time domain experiments to achieve an equivalent pulse energy.) A clear difference in the time and frequency domain data is the way in which the inter-

ference of the resonant and non-resonant contribution manifests itself. As can be seen from Fig. 3 in the frequency domain data the whole spectral region is affected, whereas in the time domain measurement interference occurs over a limited time only.

In the time domain experiments, super-imposed on the exponential decay, small oscillations in the amplitude can be observed. The period of these oscillations is 500 ± 50 fs, which corresponds to a frequency difference of 64 ± 6 cm^{-1} . These oscillations can be attributed to interference between the vibrational coherence of the symmetric C–H stretch mode and the vibrational coherence of the asymmetric stretch vibration (the difference in frequency is 61 cm^{-1} , see Fig. 3) in agreement with previous observations [21].

The shape of the frequency domain spectrum shows that the resonant and non-resonant sum frequency fields are comparable in size and that interference seems to be constructive. In other studies, in particular experimental [23] and theoretical [24] sum and difference frequency generation studies of CN^- ions adsorbed on a gold electrode, it was observed that the non-resonant signal is much larger than the resonant signal and that interference is destructive for SFG measurements (causing the signal to appear as a dip) and constructive for DFG measurements (causing the signal to appear as a positive peak). This discrepancy can be explained by noting that in our case both resonant and non-resonant signal are of comparable size. An apparent constructive interference might also be a destructive one in which the magnitude of the resonant signal is larger than the non-resonant one. The reason for such a small non-resonant signal lies in the fact that the non-resonant signal from the gold film has its origin in two types of source currents: a surface current that is generated in the first few Ångströms of the film and a bulk current that extends into the metal for approximately one optical skin depth (~ 10 nm) [25,26]. In our case the film thickness is well below the skin depth, so that the second current source contributes only slightly to the emitted non-resonant SFG field. Apparently, the contribution to the SFG signal from bulk sources is significant for SFG from gold.

5. Inhomogeneous broadening

In the previous section we have established that for the methyl (CH_3) stretch vibration of acetonitrile the SFG formalism as outlined in Section 2 works well and that there is a homogeneous distribution of resonance frequencies. Very contrasting behavior is observed for the C–N stretch vibration of acetonitrile on gold. Fig. 4 shows both the SFG spectrum (top panel) and the FID (bottom panel) of the C–N stretch vibration. The SFG spectrum

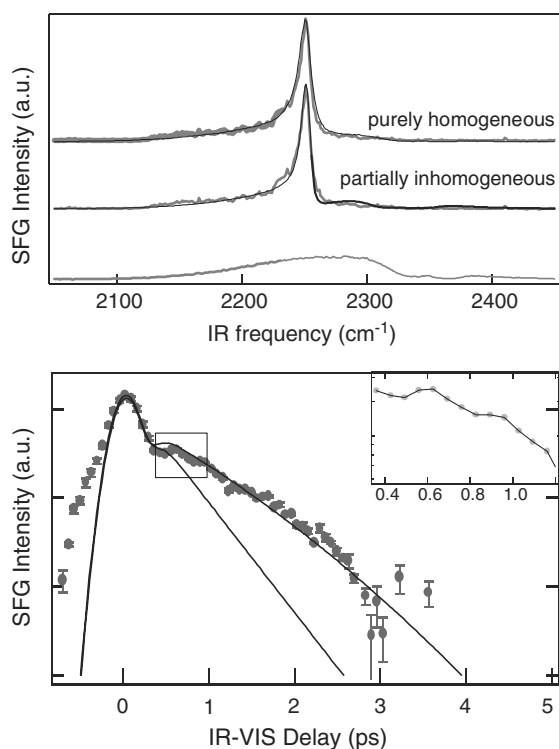


Fig. 4. Top panel: SFG spectra in the C–N stretch region of a gold film in contact with acetonitrile. The fit in the upper trace is a fit using Eqs. (4) and (5). The fit in the middle trace incorporates inhomogeneous broadening and is described in the text. The gold/ CaF_2 air spectrum is also shown, in which the degenerate asymmetric stretch vibration of CO_2 appears clearly. Bottom panel: Free induction decay (on a log scale) of the C–N stretch vibration on a log scale. The solid lines are calculations assuming homogeneous (decaying exponentially) and partial inhomogeneous broadening (the fit through the data) using the same parameters as in the top panel. The inset shows the oscillations in the free induction decay in the region highlighted by the box.

shows one vibrational resonance at 2250 cm^{-1} , which corresponds to the C–N stretch vibration. The non-resonant gold/air spectrum is also shown. It shows two dips that are caused by IR absorption lines of CO_2 present in ambient air between 2300 and 2400 cm^{-1} .

The free induction decay of the C–N stretch mode displays oscillations at small delay times (between 0 and 1 ps, see the inset in the lower panel). These weak oscillations have a period of $\sim 320\text{ fs}$ corresponding to a frequency difference of 104 cm^{-1} . A frequency difference of 104 cm^{-1} with respect to the C–N resonance frequency does not correspond to any known vibrational resonance of acetonitrile. It does correspond however, to the difference between the frequency of the C–N stretch vibration and the frequency of the asymmetric degenerate CO_2 stretch vibration. As part of the IR field is resonant with the asymmetric degenerate CO_2 stretch vibration, it sets up an IR polarization in air (before arriving at the sample) that radiates an IR electromagnetic field and interferes with the original field which then becomes slightly modulated, resulting in modulations of the non-resonant SFG field. Between approximately 0 and 1 ps there is significant interference between the resonant and non-resonant sum frequency field and hence oscillations will appear in the signal (without affecting the overall decay of the resonant contribution).

The frequency domain spectrum can be reproduced very well with Eqs. (4) and (5), using $\omega_{0n} = 2250\text{ cm}^{-1}$ and $\Gamma = 7.6\text{ cm}^{-1}$ ($T_2 = 0.68\text{ ps}$). As mentioned in Section 2, both the SFG spectrum and the FID are a measurement of the same polarization, so that the FID should be described with the time domain equivalent (Fourier transform) of the frequency domain response. However, an exponentially decaying $\chi_{\text{RES}}^{(2)}(t)$ with $T_2 = 0.68\text{ ps}$ (the exponential FID, shown in the lower panel of Fig. 4) clearly does not describe the measured FID. Inversely, an exponential fit to the time domain measurement results in a frequency domain FWHM linewidth of 6.6 cm^{-1} , which is significantly too narrow. Apparently, obtaining a good fit with the commonly employed Eq. (3) is not a guarantee for homogeneous dephasing behavior.

The clearly non-exponential decay of the FID seems to suggest a partially inhomogeneous scenario, in which the resonance frequency is not the same for all molecules but varies with the adsorption site. Following Refs. [27,5,28], such a partially inhomogeneous distribution of adsorption sites can be characterized by a Gaussian distribution, $g(\omega'_{0n})$, of resonance frequencies (ω'_{0n}) centered around ω_{inh} with a width $\Delta\omega$, i.e. $g(\omega'_{0n}) = \frac{2}{\Delta\omega\sqrt{\pi}} e^{-(\omega'_{0n}-\omega_{inh})^2/(\Delta\omega)^2}$. The time domain resonant response can then be written as:

$$\begin{aligned}\chi_{RES}^{(2)}(t) &= \sum_{\omega'_{0n}} \chi_{RES}^{(2)}(t, \omega'_{0n}) \\ &= \int_0^\infty d\omega'_{0n} g(\omega'_{0n}) e^{-t/T_2} e^{i(\omega'_{0n} + \omega_1)t} \\ &\equiv \bar{\chi}_{RES}^{(2)}(t) \cos(\omega_{inh} + \omega_1)t,\end{aligned}\quad (6)$$

which consists of a time dependent envelope $\bar{\chi}_{RES}^{(2)}(t)$ and an oscillating term with frequency $\omega_{inh} + \omega_1$. Around the sum frequency the envelope can be approximated by:

$$\bar{\chi}_{RES}^{(2)}(t) = e^{-t/T_2} e^{-t^2(\Delta\omega/2)^2} \quad (7)$$

as long as $\frac{\Delta\omega}{\omega_{inh}} \ll 1$. This is a generalized version of the commonly used equations to fit SFG spectra. If we insert a δ -function distribution of resonance frequencies, $g(\omega'_0) = \delta(\omega'_0 - \omega_0)$, the homogeneous scenario is retrieved with the response as given by Eq. (3). The amount of inhomogeneity is determined by the product $\Delta\omega T_2$; $\Delta\omega T_2 \ll 1$ describes a homogeneous scenario, whereas $\Delta\omega T_2 \gg 1$ yields a totally inhomogeneous distribution of sites. To obtain the frequency domain polarization, we take the Fourier transform of $P^{(2)}(t, \tau = 0)$ and regard the visible field as a CW field again. Applying Eqs. (1) and (2) to calculate the FID and the upper part of Eq. (4) in combination with the Fourier transform of Eq. (6) to reproduce the spectrum yields the fits to the frequency and time domain data in Fig. 4. Using the same dephasing time ($T_2 = 1.65 \pm 0.4$ ps) and frequency distribution ($\omega_{inh} = 2250$ cm^{-1} and $\Delta\omega = 2.8 \pm 1$ cm^{-1} and $\Delta\omega T_2 = 0.6$), both the SFG spectrum and the FID can be reproduced very well with one set of parameters. That this is a unique set of parameters can be seen from the functional form

of $\bar{\chi}_{RES}^{(2)}(t)$ immediately. Namely, the function in the exponent is a unique function. This directly translates to the uniqueness of $\bar{\chi}_{RES}^{(2)}(t)$ itself. To illustrate this, Fig. 5 shows three calculated SFG spectra and free induction decays for two different sets of $\Delta\omega$ and T_2 . $\Delta\omega = 2.8$ cm^{-1} and $T_2 = 1.65$ ps corresponds to the best fit. The degree of inhomogeneity, $\Delta\omega$, was varied by a factor of 2, and T_2 was treated as a fitting parameter. It clearly demonstrates that a time domain measurement allows for a more accurate estimate of T_2 and $\Delta\omega$ than a frequency domain measurement.

Thus, we can conclude that the time domain measurement is much more sensitive to the spectral line shape. This can be understood by noting that it is inherently more sensitive to the molecular response than the frequency domain measurement, since the non-resonant signal is only present for

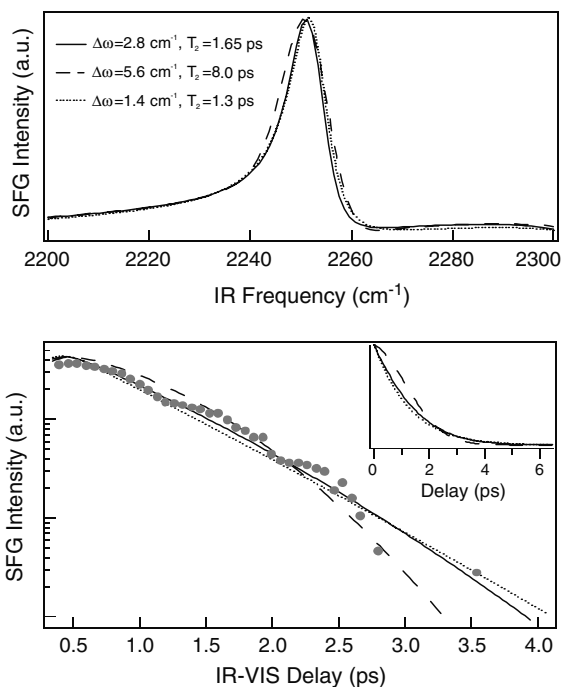


Fig. 5. Calculated frequency domain (top panel) and time domain SFG spectra (bottom panel) in the C–N stretch region of acetone for different values of $\Delta\omega$ and T_2 . The solid line corresponds to the fit in Fig. 4. $\Delta\omega = 1.4$ cm^{-1} , $T_2 = 1.3$ ps corresponds to a more homogeneous scenario (\cdots) and $\Delta\omega = 5.6$ cm^{-1} , $T_2 = 8.0$ ps corresponds to a more inhomogeneous scenario ($---$). The time domain data is also shown. The inset shows $\bar{\chi}_{RES}^{(2)}(t)$ changing shape.

the brief period of time when the two short pulses overlap. For IR-VIS delay >0.5 ps the time domain FID is governed solely by the decay of the resonant polarization. In contrast, the frequency domain SFG spectrum does not give an unobscured image of the resonant polarization, since the molecular polarization interferes with the non-resonant metal response over the whole spectral region. Therefore, independent of the line shape model employed, a theoretical description of the frequency domain data will always have one extra parameter, namely the phase difference between the resonant and non-resonant response. Apart from an extra fitting parameter, the frequency domain SFG spectra can also be distorted due to the large dispersion in the refractive index of acetonitrile around the resonance [10]. This effect will be present in the interference region and hence can cause appreciable distortion to the frequency domain spectrum. Moreover, from an experimental point of view, the signal-to-noise in the time domain experiment can be increased more easily than the signal-to-noise in the frequency domain experiment. Thus, although frequency domain and time domain SFG experiments are theoretically equivalent, they can lead to different conclusions concerning the line shape. To elucidate the vibrational decay mechanism both time and frequency domain measurements should be conducted and analyzed in a detailed fashion.

6. The influence of the surface

Now that we have established that there is a difference in line broadening for the C–H and C–N stretch modes of acetonitrile, we can examine the role of the gold surface more closely by comparing the liquid phase infrared spectra of acetonitrile to the acetonitrile/gold spectra (see Fig. 6). The infrared spectra in Fig. 6 display vibrational resonances corresponding to the C–N stretch mode at 2253 cm^{-1} and resonances corresponding to the symmetric and asymmetric CH_3 stretch modes at 2946 cm^{-1} and 3002 cm^{-1} . From the Lorentzian fits we obtain linewidths (Γ) of 8.7 cm^{-1} (corresponding to 0.61 ps) for the symmetric stretch vibration, 26.6 cm^{-1} (corresponding to 0.20 ps) for the asym-

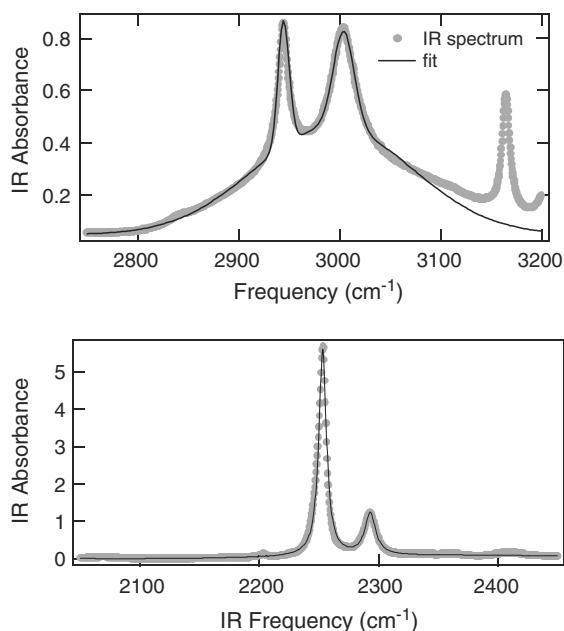


Fig. 6. IR spectra of a $15\text{ }\mu\text{m}$ thick film of acetonitrile in the C–H stretch (top panel) and the C–N stretch (bottom panel) spectral regions. The solid lines are fits assuming Lorentzian line shapes, implying homogeneous line broadening. The band at $\sim 3150\text{ cm}^{-1}$ is a combination mode of the C–C and the C–N stretch vibrations and the band at $\sim 2287\text{ cm}^{-1}$ is an overtone of the C–H rocking mode [30].

metric stretch vibration and 3.9 cm^{-1} for the symmetric stretch vibration. For both the C–H and C–N stretch modes the obtained resonance frequencies and linewidths from the bulk liquid do not differ very much from the ones we have observed with SFG. This means that the effect the gold surface has on the acetonitrile molecules is marginal.

It has been shown that if the CH_3 group were pointing down to the surface, the vibrational frequency would be red-shifted [29]. The absence of a frequency shift indicates that acetonitrile molecules point with their C–N end towards the surface. Unlike many other molecules that have been studied on various surfaces with SFG, it is impossible in this system to determine the average orientation of molecules from comparing the amplitude of SFG spectra at various polarization combinations. The procedure of finding the molecular orientation, as described in Ref. [13], requires an appropriate distribution function of

the molecules at surface layer. Due to the high degree of surface corrugation, it is impossible to accurately determine the distribution function and we cannot just assume that all the molecules are distributed under a certain angle on a flat surface.

The infrared spectra of liquid acetonitrile can be described very well using Lorentzian line shapes, which indicates homogeneous line broadening for both the C–N stretch vibration and the C–H stretch vibrations in liquid acetonitrile. The observed partial inhomogeneity for the C–N stretch vibration can be concluded to be imposed by the surface and not due to any ordering already present in the liquid phase. The surface roughness (displayed in Fig. 2) leads to the appearance of different adsorption sites, resulting in an inhomogeneous distribution of vibrational resonances for the vibrational mode that is closest to the surface.

7. Conclusions

We have shown it is possible to study molecules absorbed onto a very thin gold film using femto-second sum frequency generation. By applying time and frequency domain sum frequency generation, we have found that, although both measurement schemes are theoretically equivalent, they can lead to different conclusions concerning the line shape. To elucidate the vibrational decay mechanism both time and frequency domain measurements should be conducted and analyzed in a detailed fashion. The effect of the gold surface on acetonitrile is a marginal one, resulting only in the inhomogeneity of vibrational mode that is closest to the surface (the C–N stretch mode).

Acknowledgments

The authors would like to thank R.C.V. van Schie and P. Schakel for excellent technical support. This work is part of the research program of the “Stichting voor Fundamenteel Onderzoek der Materie (FOM)”, which is financially supported by the “Nederlandse organisatie voor Wetenschappelijk Onderzoek (NWO)”.

References

- [1] G.A. Somorjai, *Chemistry in Two Dimensions: Surfaces*, Cornell University Press, New York, 1981.
- [2] G. Ertl, *Faraday Discuss.* 121 (2002) 1.
- [3] G.R. Bell, Z.X. Li, C.D. Bain, P. Fisher, D.C. Duffy, *J. Phys. Chem. B* 101 (1998) 9461.
- [4] Y.R. Shen, *The Principles of Nonlinear Optics*, Wiley, New York, 1984.
- [5] P. Guyot-Sionnest, *Phys. Rev. Lett.* 66 (1991) 1489.
- [6] S. Roke, A.W. Kleyn, M. Bonn, *Chem. Phys. Lett.* 370 (2003) 227.
- [7] H. Ueba, T. Sawabu, T. Mii, *Surf. Sci.* 502–503 (2002) 254.
- [8] J.C. Owrutsky, J.P. Culver, M. Li, Y.R. Kim, M.J. Sarisky, M.S. Yeganeh, A.G. Yodh, R.M. Hochstrasser, *J. Chem. Phys.* 97 (1992) 4421.
- [9] E. van der Ham, Ph.D. Thesis, Leiden University, Faculty of Mathematics and Natural Sciences, 1998.
- [10] C.T. Williams, Y. Yang, C.D. Bain, *Langmuir* 16(2000)2343.
- [11] J.H. Hunt, P. Guyot-Sionnest, Y.R. Shen, *Chem. Phys. Lett.* 133 (1987) 189.
- [12] P. Guyot-Sionnest, J.H. Hunt, Y.R. Shen, *Phys. Rev. Lett.* 59 (1989) 1597.
- [13] X. Zhuang, P.B. Miranda, D. Kim, Y.R. Shen, *Phys. Rev. B* 59 (1999) 12632.
- [14] R. Kubo, M. Toda, N. Hashitsume, *Statistical Physics II*, Springer-Verlag, Berlin, 1995.
- [15] E.W.M. van der Ham, Q.H.F. Vreken, E.R. Eliel, *Surf. Sci.* 386 (1996) 96.
- [16] L.J. Richter, T.P. Petralli-Mallow, J.C. Stephenson, *Opt. Lett.* 23 (1998) 1594.
- [17] T. Mii, H. Ueba, *Surf. Sci.* 427 (1999) 324.
- [18] T. Ishibashi, H. Onishi, *Chem. Phys. Lett.* 346 (2001) 413.
- [19] S.R. Hatch, R.S. Polizzotti, S. Dougal, P. Rabinowitz, *Chem. Phys. Lett.* 196 (1992) 97.
- [20] M. Bonn, D.N. Denzler, S. Funk, M. Wolf, S.-S. Wellershof, J. Hohlfeld, *Phys. Rev. B* 61 (2000) 1101.
- [21] D. Star, T. Kikteva, G.W. Leach, *J. Chem. Phys.* 111 (1999) 14.
- [22] M. Saß, M. Lettenberger, A. Lauberau, *Chem. Phys. Lett.* 356 (2002) 284.
- [23] A.L. Rille, A. Tadjeddine, W.Q. Zheng, A. Peremans, *Chem. Phys. Lett.* 271 (1997) 95.
- [24] B.S. Mendoza, W.L. Mochán, J.A. Maytorena, *Phys. Rev. B* 60 (1999) 14334.
- [25] J. Rudnick, E.A. Stern, *Phys. Rev. B* 4 (1971) 4274.
- [26] A.V. Petukhov, V.L. Brudny, W.L. Mochán, J.A. Maytorena, B.S. Mendoza, T. Rasing, *Phys. Rev. Lett.* 81 (1998) 566.
- [27] C.D. Bain, P.B. Davies, T.H. Ong, R.N. Ward, M.A. Brown, *Langmuir* 7 (1991) 1563.
- [28] M. van der Voort, C.W. Rella, L.F.G. van der Meer, A.V. Akimov, J.I. Dijkhuis, *Phys. Rev. Lett.* 84 (2000) 1236.
- [29] S. Baldeli, G. Mailhot, P. Ross, Y.R. Shen, G.A. Somorjai, *J. Phys. Chem. B* 105 (2001) 654.
- [30] G. Herzberg, *Molecular Spectra and Molecular Structure II*, D. Van Nostrand Company, Princeton, 1945.